Atomic force microscope tip-induced local oxidation of silicon: kinetics, mechanism, and nanofabrication

Phaedon Avouris,[a] Tobias Hertel, and Richard Martel
IBM Research Division, T. J. Watson Research Center, Yorktown Heights, New York 10598

(Received 21 April 1997; accepted for publication 12 May 1997)

Atomic force microscope induced local oxidation of silicon is a process with a strong potential for use in proximal probe nanofabrication. Here we examine its kinetics and mechanism and how such factors as the strength of the electric field, ambient humidity, and thickness of the oxide affect its rate and resolution. Detection of electrochemical currents proves the anodization character of the process. Initial very fast oxidation rates are shown to slow down dramatically as a result of a self-limiting behavior resulting from the build up of stress and a reduction of the electric field strength. The lateral resolution is determined by the defocusing of the electric field in a condensed water film whose extent is a function of ambient humidity. © *1997 American Institute of Physics.* [S0003-6951(97)03628-0]

There is currently great interest in the possible use of proximal probes as tools for the fabrication of nanoelectronic devices. Among the different approaches tested so far, the most promising has been the atomic force microscope (AFM) induced oxidation of silicon and metals. The first report of tip-induced oxidation of silicon was a scanning tunneling microscope (STM) study by Dagata *et al.*[1] In this study, an H-passivated Si surface was scanned in air by a *positively* biased tip to generate surface oxide features. A different approach, where an AFM with a conducting tip biased *negative* with respect to the sample is used to induce oxidation, was demonstrated by a number of workers.[2–5] With this approach, thicker insulating oxides can be produced. Oxide lines as narrow as 10 nm have been generated,[4] and nanoelectronic devices have been fabricated using this process.[6–9] The mechanism of the tip-induced oxidation has been addressed by several authors. The dependence of the tip-induced oxidation on tip bias provides evidence that the process is affected by the generated electric field. Furthermore, Gordon *et al.*[10] suggested that the initial density of surface OH groups is rate limiting, while Teuschler *et al.*[11] attempted, unsuccessfully, to explain the tip-induced oxidation in terms of the Cabrera and Mott model[12] of field-induced oxidation. The fact that water from the ambient is necessary for the oxidation has been interpreted by Sugimura *et al.*[13] as an indication that the process is analogous to electrochemical anodization. No current flow has, however, been detected during the reaction.

To optimally use this oxidation process in nanofabrication requires that we understand the factors that control its characteristics. With this in mind, we address questions involving the mechanism of the process, the rate of the reaction, and its dependence on electric field strength and oxide thickness, and try to identify the factors that control the thickness and lateral extent of the oxide, (i.e., the lithographic resolution).

The *n*-type (8–12 Ω cm) Si(100) samples were cleaned by removal of the native oxide in aqueous 10% HF solution. Local oxidation was performed in the ambient using conducting p^{++}-Si tips (radius <100 Å) and a commercial AFM microscope (M5, Park Scientific Instruments). The relative humidity was kept constant during experiments at values ranging from 10% to 95%.

In Figs. 1(a) and 1(b), we show two grids of oxide lines written at a rate of 0.3 μm/s using -10 V tip bias. In Fig. 1(a), the relative humidity was 61% and the linewidth $\sim$90 nm. Lowering the humidity to 14% reduces the width by a factor of $\sim$4. The height of the oxide barely changes. Such results demonstrate the strong influence of external factors on the characteristics of the oxidation process. One of the most important pieces of information needed in considering the use of the process in fabrication is its intrinsic rate. To determine the reaction kinetics, we applied voltage pulses with the tip stationary over a surface site. The applied voltage was then varied between -2 and -20 V and the pulse duration was increased from 10 ms to 1000 s while the tip was moved to a new position before each pulse. The width and height of the resulting oxide dots was obtained from AFM images. To obtain the total amount of Si oxidized, we also imaged the indentations left after the oxide was selectively etched away by aqueous HF. In this way, we found an apparent volume expansion upon oxidation of 3.0 ± 0.4, which is higher than the expected increase by a factor of 2.27 anticipated for formation of amorphous SiO_2.

Kinetic results are shown in Fig. 2(a) where the height of the oxide dots is plotted versus voltage pulse duration t. The fits show a rapid decrease of the growth rate with time as $1/t$. No clear bias threshold was observed. For sufficiently

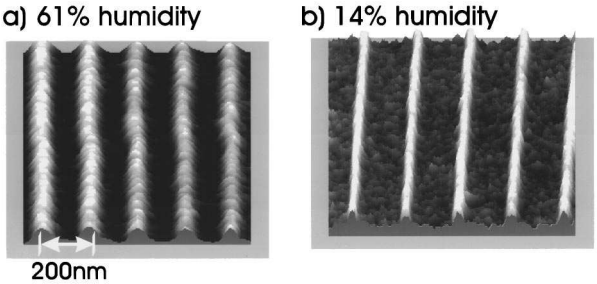

FIG. 1. The aspect ratio (height/width) of oxide lines improves significantly when the relative humidity is lowered from 61% to 14%.

[a]Electronic mail: avouris@watson.ibm.com

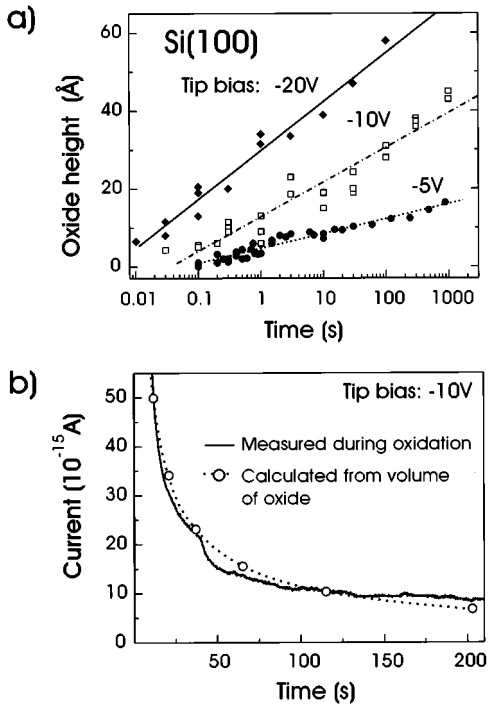

FIG. 2. (a) Kinetics of oxide dot growth for different tip bias at ~50% humidity. (b) Current measured during the oxidation process.

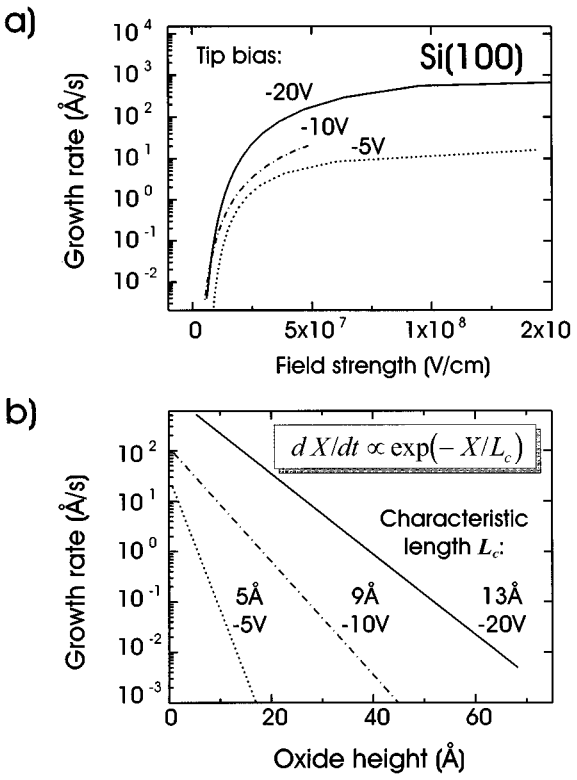

FIG. 3. (a) The growth rate versus electric field strength at the tip apex. (b) Growth rate versus oxide height at three tip biases.

long pulses, growth of shallow oxides was observed even at -2 V.

The bias dependence of the rates is a clear indication that the electric field plays an important role in the process. The high initial growth rates occur at extreme electric field strengths near the tip apex of up to $\sim 10^8$ V/cm. Field enhanced thin film oxidation was first modeled by Cabrera and Mott.[12] In their model, the role of the electric field is to lower the activation barrier for transport of ionic species across the oxide. The decrease of the growth rate observed here would then be attributed to the reduction of the electric field strength as the oxide thickness increases. To confirm the involvement of ionic species in the tip-induced oxidation process, we searched for the weak Faraday currents expected. The measured current in Fig. 2(b) shows the same behavior as the Faraday current expected for anodic oxidation if calculated from the measured volume growth according to the electrochemical reaction: $Si+4h^+ + 2OH^- \rightarrow SiO_2 + 2H^+$. Here the charge efficiency was ~50%. This efficiency, however, varies from experiment to experiment, probably due to oxide formed at the tip apex and differences in surface passivation.

From the straight line fits in Fig. 2(a), we obtain the growth rate as a function of electric field strength [Fig. 3(a); here we assumed that the entire potential drops across the oxide]. The high initial rates ($\sim 10^3$ Å/s for -20 V) decrease fast with decreasing field strength and the oxide practically ceases to grow at field strengths $< 1 \times 10^7$ V/cm. Furthermore, it is evident that the rate of oxidation is not only a function of electric field strength but also depends on the applied bias—in particular for high fields. From this, we see that the simple Cabrera–Mott model alone cannot account for the observed kinetics. This becomes even more evident when the oxidation rate is plotted versus oxide thickness [Fig. 3(b)]. If the kinetics were to obey the Cabrera–Mott model, the data should not fall on a straight line as seen from the graph because the Cabrera–Mott rate constant is proportional to $\exp(qa\Delta\Phi/2XkT)$. Here, q is the charge of moving ions, a gives the distance between interstitial sites of ions, $\Delta\Phi$ is the potential drop across the oxide, and X the oxide thickness. Deviations from Cabrera–Mott type kinetics are also observed in thermal oxide growth. This is partly attributed to the influence of stress, σ, on the oxidation rates. Large stresses build up during oxidation due to the large volume mismatch $V_{Si}/V_{SiO_2} = 20$ Å^3/45 Å^3 between Si and SiO_2. The stress should increase the activation energy for oxidation because of the work that has to be done due to the volume expansion ΔV^+ in the transition state. The reaction rate may be written as $k_S = k_0 \exp(-\sigma \Delta V^+/kT)$, where k_0 gives the rate in the absence of stress. During thermal Si oxidation at temperatures above 800 °C, stress is relieved by the viscous flow of SiO_2. This is reflected in an increase of the characteristic decay length L_c from 8 to 12 Å when the temperature is raised from 800 to 1000 °C.[14] However, in our room temperature experiments—where SiO_2 cannot flow—we observe a similar trend and the characteristic lengths increase from 5 to 13 Å when the tip bias is raised from -5 to -20 V [Fig. 3(b)]. Thus, for a given oxide thickness, the higher bias (and thus stronger electrical field) not only leads to higher growth rates but also increases L_c. This suggests that the electric field may also contribute to strain relaxation. Possible field enhanced strain relief mechanisms include silicon out diffusion through the oxide, and defect formation in the oxide. The discrepancy between the observed volume expansion of 3.0 instead of 2.27 may be an

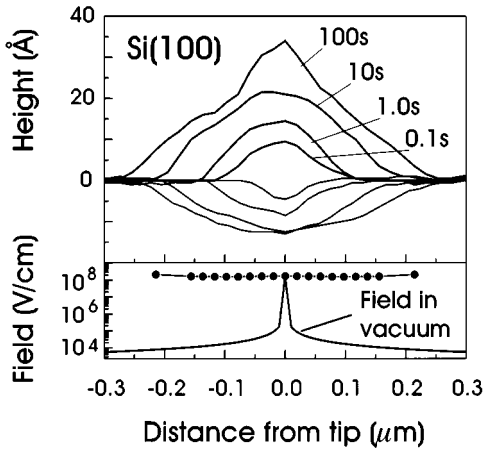

FIG. 4. Profiles of oxide dots grown at -10 V tip bias. Lower panel: The calculated electric field for a tip 30 Å in front of a conducting surface in vacuum (solid line) and the field calculated from the observed growth rate (solid circles). High growth rates at the edges of the dots show that the field is strongly defocused by the water film on the oxide.

indication that the high strains are relieved by the formation of a rather open and defect-rich oxide.

The details of the reaction kinetics—which are not very well understood even in the case of thermal oxidation—should be further influenced by the field dependence of the concentration of reactant species and their solubility in the oxide. Nevertheless, it is evident that the self-limiting oxide growth puts clear limitations on the use of this process as a high speed lithographic tool, a fact that can only be partially compensated for by the use of multiple writing tips.

To determine what parameters affect the lateral resolution of the oxidation process, we investigated the lateral growth kinetics using oxide dot profiles (Fig. 4). The strong field dependence of the oxidation kinetics, together with the anticipated focusing of the electric field at the tip apex (radius <100 Å) should, in principle, allow to pattern very narrow oxide structures. However, the increase of oxide height in Fig. 4 is nearly constant over the whole dot when going from 10 to 100 s pulse duration, for example. If we calculate (based on the observed growth at the tip apex) the electric field strength required to obtain this growth rate, we find that the field strength across the oxide must be roughly constant even at large distances from the tip. This contradicts with the field distribution expected for a tip in front of a conducting surface in vacuum (Fig. 4). The latter would decay approximately inversely proportional with the distance from the tip. We attribute this behavior to the finite electrical conductance of the water film that forms between hydrophilic (oxidized) regions of the surface and the tip apex. Direct evidence for the presence of such a film is provided by force versus distance curves (not shown). As in an electrochemical environment, the electric potential should be nearly constant within the water film and will drop in the proximity of the electrode solvent interface, i.e., in the electrochemical double layer. The extent of the water film which ''defocuses'' the electric field thus plays a decisive role in the resolution of the process. The formation and extent of this film is governed by a number of factors including capillary forces, high electric field gradients at the tip apex, the wetting behavior of the substrate and the tip and the relative humidity. In this respect, writing with *hydrophobic* carbon nanotubes appears promising and preliminary experiments have shown improved resolution. The effect of the ambient humidity can also be seen in Fig. 1 where the resolution is significantly enhanced at lower humidity. We furthermore note that the stress which develops during the oxidation also favors oxides with low curvature,[15] i.e., shallow oxides. By increasing the field strength, thicker oxides (e.g., >100 Å) can be grown but with a decreasing aspect ratio.

In summary, we have investigated the kinetics and electric field dependence of AFM induced local oxidation of Si(100) in air. The ultrasmall currents we measured during oxidation show that the oxidizing species are ionic, presumably OH^-, from the water film on the oxide. The rate of oxidation was found to decrease rapidly as the oxide film grows due to the self-limiting influence of decreasing field strengths and the buildup of stress. The water film condensed on the surface not only supplies the oxidizing species, but its finite conductance also leads to a defocusing of the electric field, which degrades the lateral resolution of the process.

The authors would like to acknowledge the contributions of B. Ek, R. Rouse, and R. Sandstrom. T.H. acknowledges financial support by the Alexander von Humboldt foundation and the Max–Planck Society. R.M. is thankful for a F.C.A.R. postdoctoral fellowship.

[1] J. A. Dagata, J. Schneir, H. H. Harary, C. J. Evans, M. T. Postek, and J. Bennett, Appl. Phys. Lett. **56**, 2001 (1990).
[2] H. C. Day and D. R. Allee, Appl. Phys. Lett. **62**, 2691 (1993).
[3] M. Yasutake, Y. Ejiri, and T. Hattori, Jpn. J. Appl. Phys. **32**, L1021 (1993).
[4] E. S. Snow and P. M. Campbell, Appl. Phys. Lett. **64**, 1932 (1994).
[5] T. Hattori, Y. Ejiri, K. Saito, and M. Yasutake, J. Vac. Sci. Technol. A **12**, 2586 (1994).
[6] S. C. Minne, H. T. Soh, Ph. Flueckiger, and C. F. Quate, Appl. Phys. Lett. **66**, 703 (1995).
[7] E. S. Snow and P. M. Campbell, Science **270**, 1639 (1995).
[8] K. Matsumoto, S. Takahashi, M. Ishii, M. Hoshi, A. Kurokawa, S. Ichimura, and A. Ando, Jpn. J. Appl. Phys. **34**, 1387 (1995).
[9] Ph. Avouris *et al.*, in *The Physics of Semiconductors*, edited by M. Scheffler and R. Zimmermann (World Scientific, Singapore, 1996), Vol. 1, pp. 51–58.
[10] A. E. Gordon, R. T. Fayfield, D. D. Litfin, and T. K. Higman, J. Vac. Sci. Technol. B **13**, 2805 (1995).
[11] T. Teuschler, K. Mahr, S. Miyazaki, M. Hundhausen, and L. Ley, Appl. Phys. Lett. **67**, 3144 (1995).
[12] N. Cabrera and N. F. Mott, Rep. Prog. Phys. **12**, 163 (1949).
[13] H. Sugimura, T. Uchida, N. Kitamura, and H. Masuhara, J. Phys. Chem. **98**, 4352 (1994).
[14] H. Z. Massoud, J. D. Plummer, and E. A. Irene, J. Electrochem. Soc. **132**, 2685 (1985).
[15] D.-B. Kao, J. P. McVittie, W. D. Nix, and K. C. Saraswat, IEEE Trans. Electron Devices **35**, 25 (1988).